

## Simplified stress-strain model for circular steel tube confined UHPC and UHPFRC columns

An H. Le <sup>\*1,2</sup>, Fehling Ekkehard <sup>3a</sup>, Duc-Kien Thai <sup>4b</sup> and Chau V. Nguyen <sup>5c</sup>

<sup>1</sup> Division of Construction Computation, Institute for Computational Science, Ton Duc Thang University, Ho Chi Minh City, Vietnam

<sup>2</sup> Faculty of Civil Engineering, Ton Duc Thang University, Ho Chi Minh City, Vietnam

<sup>3</sup> Faculty of Civil and Environmental Engineering, Institute of Structural Engineering, University of Kassel, Germany

<sup>4</sup> Department of Civil and Environmental Engineering, Sejong University, 98 Gunja-dong, Gwangjin-gu, Seoul, 143-747, South Korea

<sup>5</sup> Institute of Research and Development, Duy Tan University, 03 Quang Trung, Danang, Vietnam

(Received June 4, 2018, Revised July 30, 2018, Accepted August 1, 2018)

**Abstract.** The research on the confinement behavior of ultra high performance concrete without and with the use of steel fibers (UHPC and UHPFRC) has been extremely limited. In previous studies, authors experimentally investigated the axially compressive behavior of circular steel tube confined concrete (STCC) short and intermediate columns with the employment of UHPC and UHPFRC. Under loading on only the concrete core, the confinement effect induced by the steel tube was shown to significantly enhance the ultimate stress and its corresponding strain of the concrete core. Therefore, this paper develops a simplified stress – strain model for circular STCC columns using UHPC and UHPFRC with compressive strength ranging between 150 MPa and 200 MPa. Based on the regression analysis of previous test results, formulae for predicting peak confined stress and its corresponding strain are proposed. These proposed formulae are subsequently compared against some previous empirical formulae available in the literature to assess their accuracy. Finally, the simplified stress – strain model is verified by comparison with the test results.

**Keywords:** UHPC; UHPFRC; steel tube; STCC columns; confinement effect; stress-strain model

### 1. Introduction

It is well known that concrete filled steel tube (CFST) columns, which consist of a hollow steel tube column infilled with concrete, has been widely applied to bridges, high rise building and support structures due to their construction efficiency such as high strength and ductility, large stiffness, large energy dissipation capacity, high fire resistance, and rapid construction (Han *et al.* 2014, Giakoumelis and Lam 2004, Ellobody *et al.* 2006). In practice, there are usually two loading patterns applied to CFST columns to exploit the structural benefits from the composite action of two materials: (1) loading on the entire section and (2) loading on only the concrete core. Under axial loading on the entire section, the external steel tube in CFST columns can act as both longitudinal and transverse reinforcement, which provides both axial resistance together with the concrete core and lateral confining pressure to the concrete core. The confinement effect induced by the steel tube leads to a significant increase in both strength and ductility for CFST columns. However, when the load is applied to only the concrete core, steel tube

carries less axial load and mainly provides lateral confining pressures to the concrete core, thus causing a maximal confinement effect. It should be noted that CFST columns subjected to the load on the concrete core refer to a form of steel tube confined concrete (STCC) columns (Han *et al.* 2005, 2008, Yu *et al.* 2010, An and Fehling 2017d). Previous studies have indicated that STCC columns exhibit some advantages over the conventional CFST columns under loading on the entire section, such as higher strength and ductility, reduced possibility of steel tube buckling and shear failure, reduced complexity of connecting reinforced concrete beams to the columns (Aboutaha and Machado 1998, Johansson 2002, An and Fehling 2017d, Han *et al.* 2005, 2008). In terms of CFST and STCC columns, circular section has received a large amount of research attention because the use of this shape leads to the most effective confinement for the whole cross section, as compared to other shapes (i.e., square, rectangular sections). It has been found in the literature that the majority of previous studies have been focused on the CFST columns, while very little attention has been paid to STCC columns.

In recent times, there has been an accelerating interest in the use of ultra high performance concrete (UHPC) in construction throughout the world. This is attributed to the fact that UHPC is an advanced cementitious composite material with superior properties such as extremely high compressive strength (over 150 MPa), very high tensile strength (over 5 MPa), and very high modulus of elasticity, remarkable durability and long-term stability. UHPC has been considered as an attractive alternative to normal

\*Corresponding author, Ph.D.,  
E-mail: [lehoangan@tdtu.edu.vn](mailto:lehoangan@tdtu.edu.vn)

<sup>a</sup> Professor

<sup>b</sup> Assistant Professor

<sup>c</sup> Ph.D.

strength concrete (NSC) and high strength concrete (HSC) in constructions. Despite the above advantages, there has been hesitation in the application of UHPC due to concerns on its inherent brittleness which comes along with its very high compressive strength. Therefore, it has been advocated to confine UHPC columns with the steel tube because the confinement effect provided by the steel tube can restrict the brittleness of UHPC and increase both strength and ductility for the column (Tue *et al.* 2004b, Liew and Xiong 2012, An and Fehling 2017d). As one of the most common types of UHPC, reactive powder concrete (RPC) confined in circular stainless steel tubes was practically used for manufacturing the diagonal web members of the Sherbrooke Footbridge erected in 1997 in Canada. Blais and Couture (1999) reported that the confinement of RPC in a thin-walled stainless steel tube leads to not only a dramatic increase in the compressive strength from 200 MPa to 350 MPa but also a very high ductility for RPC. Several experimental researches have turned to the investigation on the CFST columns with the employment of UHPC. The research group led by Professor Liew conducted a comprehensive experimental campaign of 56 CFST short columns using ultra high strength concrete (UHSC) and high strength steel tube under axial compression and reported the results in some of their publications (e.g., Liew and Xiong 2010, 2012, Liew *et al.* 2014, Xiong 2012; Xiong *et al.* 2017). Likewise, the research group led by Professor Tue tested on 15 circular CFST short columns using UHPC and normal high strength steel tube under axial compression (e.g., Tue *et al.* 2004a, b, Schneider 2006). Recently, An and Fehling (2017g) presented numerical and analytical studies on the compressive behavior of circular STCC columns using UHPC with concrete cylinder strength higher than 150 MPa. These authors reached a conclusion that the ductility and strength of CFST columns using UHPC (or UHSC) can be further improved if: (1) the load is imposed only the concrete core; (2) the steel contribution ratio is increased; (3) high strength steel tube is used; (4) at least 1% volume of steel fibers is used for UHPC (or UHSC) core. The test results of these authors indicated that although circular CFST columns employing UHPC exhibit a tremendous load bearing capacity, an abrupt drop of load after the peak load usually appears in the load versus axial displacement response. In addition, unlike circular CFST columns using NSC which have a remarkable plastic deformation, circular CFST columns using UHPC were found to exhibit a small plastic deformation. These authors also pointed out that a sufficient amount of confinement is required for CFST columns using UHPC (or UHSC) to impede the sudden loss of load capacity after attaining the peak load. In fact, studies on CFST using UHPC, in general, and on STCC using UHPC, in particular, remain extremely limited. Accordingly, as one of the best solutions for improving the ductility and strength, circular STCC columns using UHPC should be further investigated to gain a deeper insight into the potential benefits of their mechanical performance. The use of fiber reinforced UHPC (UHPFRC) for filling in STCC columns should be also considered in further research for enhancing the ductility and delaying the shear failure.

It is well understood that the knowledge of stress and strain is indispensable to understand the compressive behavior of a CFST or STCC column. To establish a rational design method for concrete columns confined by steel tube, a large number of research efforts have been paid to develop accurate constitutive stress – strain models for confined concrete. In these analytical models, the enhancement of stress and strain arising from the confinement effect is quantified using proposed design formulae. It has been found that the previous analytical models for confined concrete have been mainly concerned with NSC or HSC. Moreover, most of previous analytical models have been established based on the mechanism of CFST columns under loading on the entire section, while few models have been directly built up for STCC columns. O’Shea and Bridge (2000) proposed design equations to estimate the peak confined concrete strength and its corresponding strain for circular STCC columns using NSC up to 50 MPa and HSC up to 100 MPa. Liu *et al.* (2016) presented an equation for peak confined concrete strength deriving from hoop and vertical stresses of the steel tube observed in actual tests on 29 circular STCC columns using concrete with compressive strengths varying between 30 and 80 MPa. De Oliveira *et al.* (2010) introduced a correction factor for predicting the strength of slender circular STCC columns with length-to-diameter ( $L/D$ ) ratio higher than 3. An and Fehling (2017e) developed a stress – strain relationship and formulae to predict peak confined stress and its corresponding strain for circular STCC columns made from UHPC. It has been found in the literature that studies on the stress - strain model of circular STCC columns using UHPC are extremely limited, thus highlighting the urgent need to conduct more studies on this column type.

To fulfill the research gap as outlined above, this paper is aimed at developing and simplifying a stress-strain model for circular STCC columns using UHPC and UHPFRC (STCC-UHPC and STCC-UHPFRC). To obtain this goal, the formulae for predicting peak confined stress and its corresponding strain are proposed. The proposed formulae are subsequently compared against the previous empirical formulae available in the literature in order to assess their accuracy. Finally, a simplified stress – strain relationship is also proposed and verified by comparison with test results.

## 2. Theoretical calculation of ultimate axial load and its corresponding strain of circular STCC columns

The basic formula for calculating the ultimate axial load ( $N_u$ ) of circular STCC columns was suggested by many previous studies (e.g., Yu *et al.* 2010; Guo 2014) as below

$$N_u = f_{cc} \cdot A_c = (\sigma_{cp} A_c + \sigma_v A_s) \quad (1)$$

in which  $\sigma_{cp}$  and  $\sigma_v$  are the longitudinal compressive stresses of the concrete core and the steel tube at the ultimate load  $N_u$ , respectively.  $A_c$  and  $A_s$  are the cross-sectional area of the concrete core and the steel tube, respectively.

Table 1 Formulae for predicting  $N_u$  and  $f_{cc}$  in the previous studies

Authors	Equations for $N_u$ and $f_{cc}$	Limitations	Expressions
Yu <i>et al.</i> (2010)	$f_{cc} = (1.14 + 1.34\xi)f_c$ $N_u = (1.14 + 1.34\xi)f_c \cdot A_c$	$f_y = (235 \div 345)$ MPa, $f_c = (30 \div 60)$ MPa, $\xi = 0.2-2$	
Yamamoto <i>et al.</i> (2000)	$f_{cc} = 1.67 \cdot D^{-0.112} \cdot f_c + k \frac{2t}{D-2t} f_y$		$k = 3.3$ : the value of confining factor determined empirically from the test data
O'Shea and Bridge (2000)	$\sigma_{cp} = f_c \cdot \left( -1.228 + 2.172 \cdot \sqrt{1 + \frac{7.46f_l}{f_c}} - 2 \cdot \frac{p}{f_c} \right)$ when ( $f_c \leq 50$ MPa) $\frac{\sigma_{cp}}{f_c} = \left( \frac{p}{f_t} + 1 \right)^k$ when ( $80$ MPa $\leq f_c \leq 100$ MPa) $p = p_{yield} \cdot \left( 0.7 - \sqrt{\frac{f_c}{f_y}} \right) \cdot \left( \frac{10}{3} \right)$ ; $p_{yield} = \frac{2 \cdot f_y \cdot t}{D-2t}$ ; $k = 1.25 \cdot \left( 1 + 0.062 \cdot \frac{p}{f_c} \right) \cdot (f_c)^{-0.21}$ $f_t = 0.558 \sqrt{f_c}$ and $N_u = A_c \cdot \sigma_{cp} + A_s \cdot f_y$	Equations are applicable for NSC and HSC infilled, and a wide range of $D/t$ ratio up to 200	$\sigma_{cp}$ : Compressive strength of confined concrete; $p$ : The applied confining pressure $f_y$ : Yield strength of steel $f_t$ : Tensile strength of concrete $p_{yield}$ : The confining pressure in yield condition $k$ : Parameter that reflects the effectiveness of confinement
Ding <i>et al.</i> (2011)	$N_u = \left( 1 + \frac{k \cdot \xi}{2} \right) \cdot f_c \cdot A_c$	$f_c = 30 \div 120$ MPa $D/t \geq 20$	$k = 3 \div 4.3$
Liu <i>et al.</i> (2009)	$N_u = \sigma_v A_s + \sigma_{cp} A_c$ ; $\sigma_v = 1658 (D/t)^{-0.54}$ $\sigma_{cp} = f_c \left( -1.254 + 2.254 \sqrt{1 + \frac{7.94\sigma_r}{f_c}} - 2 \frac{\sigma_r}{f_c} \right)$	$22 \leq D/t \leq 50$	$\sigma_r$ : confining pressure $\sigma_v, \sigma_{cp}$ : longitudinal stress of the steel tube and the concrete core at the ultimate state, respectively
Liu <i>et al.</i> (2016)	$N_u = \sigma_v A_s + \sigma_{cp} A_c$ ; $\sigma_v = 0.61 f_y$ ; $\sigma_h = 0.54 f_y$ $\sigma_{cp} = f_c + 4.1 \sigma_r$ ; $\sigma_r = \frac{2t \sigma_h}{D-2t} = \frac{1.08 f_y}{D}$	$D/t = 13.6 \div 586.1$ $f_c = 8.5 \div 132$ MPa	
Huang <i>et al.</i> (2012)	$N_u = (f_c + 35) \frac{1}{\gamma_c} \sqrt{\frac{A_c}{A_1}} A_1 + 0.6 A_s f_y$	Equation is applicable for NSC infilled	$A_1$ is the area below the loading plate (personal contact), $\gamma_c$ is the unit material factor
Guo (2014)	$f_{cc} = f_c (1 + \sqrt{\xi} + 1.1\xi)$ $N_u = (1 + \sqrt{\xi} + 1.1\xi) f_c \cdot A_c$	$\xi \leq 1.7$	
De Oliveira <i>et al.</i> (2010)	$N_u = (A_c f_c + A_s f_y) \lambda_{Oliveira}$ $\lambda_{Oliveira} = 1$ when $L/D \leq 3$ $\lambda_{Oliveira} = -0.18 \ln \left( \frac{L}{D} \right) + 1.2$ when $L/D > 3$	Equation is applicable for short and intermediate columns $f_c \leq 120$ MPa; $L/D = 1 \div 10$	$\lambda_{Oliveira}$ : correction factor for prediction $N_u$ of intermediate columns

The analytical expressions for the confined peak stress ( $f_{cc}$ ) and its corresponding strain ( $\varepsilon_{cc}$ ) are desirable for practically designing circular STCC columns. Several formulae have been experimentally or numerically established in the literature to estimate the values of  $f_{cc}$  and  $\varepsilon_{cc}$  in circular STCC columns (e.g., Guo 2014, Yu *et al.* 2010, De Oliveira *et al.* 2010, O'Shea and Bridge 2000, Huang *et al.* 2012, Liu *et al.* 2009, 2016, Yamamoto *et al.* 2000, Qi *et al.* 2011, Ding *et al.* 2011). Table 1 summarizes the formulae for predicting the values of  $N_u$  and  $f_{cc}$  in circular STCC short columns obtained from previous

studies. It is found that there have been generally two approaches for the prediction of  $f_{cc}$  as follows:

- The value of  $f_{cc}$  is a function of the confinement index  $\xi$ . This is attributable to the fact that the values of  $f_{cc}$  increase with the use of the higher values of  $\xi$  and this increasing rate can be described using a mathematical relationship between  $f_{cc}$  and  $\xi$ , which is usually obtained by the regression analysis from the test results.
- The value of  $f_{cc}$  is derived from the confining

Table 2 Formulae for predicting  $\varepsilon_{cc}$  in the previous studies

Authors	Equation for $\varepsilon_{cc}$	Limitations	Expressions
Guo (2014)	$\varepsilon_{cc} = 2.2\xi^{2/3} + 0.2$ ( $\varepsilon_{cc}$ in ‰)	$f_y = 235 \div 345$ MPa, $f_c = 30 \div 60$ MPa, $\xi = 0.2 \div 2$	
O'Shea and Bridge (2000)	$\varepsilon_{cc} = \varepsilon_c \left( 1 + (8 + 0.05 f_c) \left( \frac{p}{f_c} \right) \right)$	Equations are applicable for NSC and HSC infilled, and a wide range of $D/t$ ratio up to 200	Same in Table 8.2
Ding <i>et al.</i> (2011)	$\varepsilon_{cc} = (1 + 1.7\psi\xi) [1 + 3.4\sqrt{\psi\xi} A_1 - 1] \varepsilon_c$ $\varepsilon_c = 383 f_{cu}^{7/18} \times 10^{-6}$ $A_1 = 9.1 f_{cu}^{-4/9}$	$f_c = 30 \div 120$ MPa $D/t \geq 20$	$A_1$ is the variable in the ascending branch of uniaxial stress-strain relationship of unconfined concrete $\psi$ is mainly a function of concrete strength $\psi = 0.9 \div 0.0005 f_{cu}$ . $f_{cu}$ is the cubic compressive strength of concrete

pressure  $\sigma_r$ . This approach is based on a large number of confinement models for concrete which follows the well-known and the earliest works by Richart *et al.* (1928, 1929).

Furthermore, it can be apparent that the ultimate axial load  $N_u$  is mainly estimated using two methods. The first method makes use of the confinement index  $\xi$  (see Eq. (1)) to quantify the increased strength for  $N_u$  (e.g., Yu *et al.* 2010, Ding *et al.* 2011). The confinement index  $\xi$  which is well known as a key parameter to reflect the combined effect of column parameters ( $f_c, f_y, A_s, A_c$ )

$$\xi = \frac{f_y \cdot A_s}{f_c \cdot A_c} \quad (2)$$

The second method makes use of the average longitudinal compressive stress of the concrete core ( $\sigma_{cp}$ ) and the steel tube ( $\sigma_v$ ) observed from the actual test to include in the equation of  $N_u$  (e.g., O'Shea and Bridge 2000, Huang *et al.* 2012, Liu *et al.* 2009, 2016).

In general, the compressive stress of the concrete core  $\sigma_{cp}$  at the ultimate state can be given by

$$\sigma_{cp} = f_c (1 + k_{\sigma_r}) = f_c \cdot (1 + k_{\sigma_h}) \quad (3)$$

where  $k_{\sigma_r}$  and  $k_{\sigma_h}$  are the coefficients depending upon on the confining stress  $\sigma_r$  of the concrete core and the hoop stress  $\sigma_h$  of the steel tube.

From the regression analysis on test results of circular STCC columns, Guo (2014) suggested that

$$k_{\sigma_r} = 1.5 \sqrt{\frac{\sigma_r}{f_c}} + 2 \frac{\sigma_r}{f_c} \quad (4)$$

The relation between the longitudinal compressive stress  $\sigma_v$  and the hoop stress  $\sigma_h$  is determined following Von Mises criterion for the steel tube under the biaxial stress state

$$\sigma_h^2 + \sigma_v^2 + (\sigma_h - \sigma_v)^2 = 2f_y^2 \quad (5)$$

Substituting Eqs. (3)-(5) into Eq. (1), the formula for predicting  $f_{cc}$  can be simplified

$$f_{cc} = f_c \left[ 1 + k_{\sigma_h} + \xi \frac{\sigma_v}{f_y} \right] \quad (6)$$

or

$$f_{cc} = f_c [1 + \alpha \cdot \xi] \quad (7)$$

Two extreme conditions for circular STCC columns at the ultimate state can be assumed as:

- The steel tube and the concrete core reach simultaneously their individual strength, that means  $\sigma_v = f_y$  and  $\sigma_{cp} = f_c$ , while the hoop stress of the steel tube is zero ( $\sigma_h = 0$ ). Accordingly, the confining stress  $\sigma_r$  is also equal to zero ( $\sigma_r = 0$ ). Therefore, the confined peak stress  $f_{cc}$  can be taken as

$$f_{cc} = f_c (1 + \xi) \quad (8)$$

- The hoop stress of the steel tube increases to the yield strength ( $\sigma_h = f_y$ ), but the longitudinal stress of the steel tube diminishes to zero ( $\sigma_v = 0$ ). In this case, the confining stress  $\sigma_r$  becomes to be maximum, thus indicating that the coefficient  $\alpha$  in Eq. (6) reaches a maximum value  $\alpha_{\max}$ . Hence, the confined peak stress  $f_{cc}$  is given by

$$f_{cc} = f_c (1 + \alpha_{\max} \cdot \xi) \quad (9)$$

If the coefficient  $k_{\sigma_r}$  is taken as 4.1 (following the formula for predicting the confined strength of concrete in Richart 1928),  $\alpha_{\max} = 2$  is derived. From the observation of a large number of experimental studies on circular STCC columns, it can be stated that the confined peak stress  $f_{cc}$  with a certain confinement index  $\xi$  is usually between two extreme values in Eqs. (8) and (9). Similarly, the stresses in the concrete core and the steel tube vary between these two extreme conditions.

According to Japanese standard AIJ (2001), depending

Table 3 Database of circular STCC columns with UHPC and UHPFRC infilled

Authors	Specimens	$D$ (mm)	$t$ (mm)	$L_c$ (mm)	$f_c$ (MPa)	$f_y$ (MPa)	$\epsilon_c$ (%)	$\zeta$	$N_u$ (kN)	$N_{res}$ (kN)	$\epsilon_{cc}$ (%)
An and Fehing (2017a, b, c) (Short columns)	SF0-t50-L600	152.4	5.0	552.33	190.4	445.9	3.97	0.34	3645.94	3193.85	7.51
	SF1-t50-L600	152.4	5.0	548.50	195.6	445.9	4.07	0.33	3997.48	3787.56	8.01
	SF2-t50-L600	152.4	5.0	540.70	192.4	445.9	4.01	0.34	4224.02	3090.52	11.13
	SF0-t63-L600	152.4	6.3	553.00	198.0	373.4	4.12	0.36	3692.81	3165.12	7.84
	SF1-t63-L600	152.4	6.3	554.70	195.5	373.4	4.07	0.36	3807.97	2670.70	7.74
	SF2-t63-L600	152.4	6.3	552.70	187.8	373.4	3.91	0.37	4033.01	2679.52	8.74
	SF0-t88-L600	152.4	8.8	551.87	178.9	392.6	3.74	0.61	4200.84	3570.71	9.30
	SF1-t88-L600	152.4	8.8	559.67	195.5	392.6	4.07	0.56	4288.54	3564.04	11.13
Schneider (2006) (Short columns)	SF2-t88-L600	152.4	8.8	549.83	188.2	392.6	3.92	0.58	4354.06	3831.41	9.62
	NB2.5-UHFB	164.2	2.5	652.00	166.8	377.0	3.49	0.14	3501.00	2167.00	3.80
	NB3.0-UHFB	189.0	3.0	756.00	166.8	398.0	3.49	0.16	4837.00	3000.00	4.22
	NB4.0-UHFB	168.6	3.9	648.00	174.2	363.0	3.64	0.21	4216.00	2400.00	5.57
	NB4.8-UHFB	169.0	4.8	645.00	176.7	399.0	3.69	0.28	4330.00	3000.00	5.67
	NB5.0-UHFB	168.7	5.2	645.00	170.5	405.0	3.57	0.32	4715.00	3350.00	5.99
Xiong (2012) (Short columns)	NB5.6-UHFB	168.8	5.7	650.00	173.4	452.0	3.63	0.39	4930.00	3455.00	6.84
	NB8.0-UHFB	168.1	8.1	645.00	174.9	409.0	3.66	0.53	5254.00	4150.00	6.84
Xiong (2012) (Short columns)	S1-2-1(a)*	114.3	6.3	210.00	173.5	428.0	3.63	0.65	2866.00	2317.00	-
An and Fehing (2017a, b, c) (Intermediate columns)	SF0-t50-L1000	152.4	5.0	949.70	190.4	445.9	3.97	0.34	3383.35	2962.26	6.48
	SF1-t50-L1000	152.4	5.0	951.30	195.6	445.9	4.07	0.33	3724.06	2823.16	7.32
	SF2-t50-L1000	152.4	5.0	950.50	192.4	445.9	4.01	0.34	3995.71	2986.70	7.16
	SF0-t63-L1000	152.4	6.3	948.50	198.0	373.4	4.12	0.36	3861.14	2570.15	6.97
	SF1-t63-L1000	152.4	6.3	947.30	195.5	373.4	4.07	0.36	3535.31	3090.28	5.86
	SF2-t63-L1000	152.4	6.3	940.20	187.8	373.4	3.91	0.37	3584.70	2595.35	6.37
	SF0-t88-L1000	152.4	8.8	942.93	178.9	392.6	3.74	0.61	3919.86	3331.88	6.94
	SF1-t88-L1000	152.4	8.8	951.27	195.5	392.6	4.07	0.56	4178.66	3228.12	7.17
	SF2-t88-L1000	152.4	8.8	943.77	188.2	392.6	3.92	0.58	4099.79	3347.82	7.34

on the ratio of length-to-outer diameter ( $L/D$ ), CFST and STCC columns were classified as short columns ( $L/D \leq 4$ ), intermediate columns ( $4 < L/D \leq 12$ ) and slender columns ( $L/D > 12$ ). It should be noted that while the majority of the proposed formulae were concerned with the short STCC columns, there are still a lack of proposed formulae for  $N_u$  and  $f_{cc}$  in the case of the intermediate or slender STCC columns. De Oliveira *et al.* (2010) made an effort to correct the prediction of  $N_u$  for both short and intermediate columns. This correction was based on the regression analysis from 32 tested specimens of circular STCC columns covering a wide range of  $f_c$  and  $L/D$ . A correction factor  $\lambda_{Oliveira}$  was introduced for estimating the values of  $N_u$  when the circular STCC columns have  $L/D$  ratios higher than 3. Table 1 also presents the proposed formula in De Oliveira *et al.* (2010). The formulae for prediction of  $\epsilon_{cc}$  proposed by the authors who directly conducted their own studies on circular STCC stub columns are also shown in Table 2. Likewise to  $f_{cc}$ , the value of  $\epsilon_{cc}$  is predicted using the confinement index  $\zeta$  or the confining

stress  $\sigma_c$  as the main variables for considering the increased strain. Looking back again at the literature of circular STCC columns, some limitations of the proposed formulae for predictions of  $N_u$ ,  $f_{cc}$  and  $\epsilon_{cc}$  can be summarized:

- Such proposed formulae for the intermediate and slender STCC columns are still insufficient.
- The highest of concrete compressive strength adopted in the proposed formulae as mentioned above is about 120 MPa. Accordingly, there are no comprehensive formulae which cover a wide range of concrete strength up to 200 MPa and various types of concrete, especially UHPC.
- There are also no unique formulae for the case of UHPC with cylinder strength higher than 150 MPa.

For these reasons, this study conducts a regression analysis on the database of previous test results reported in Schneider (2006), Xiong (2012), An and Fehling (2017a, b, c), thereby proposing formulae to predict  $f_{cc}$  and  $\epsilon_{cc}$  of

circular STCC columns with the employment of UHPC and UHPFRC. It should be mentioned that for circular STCC columns, there are no significant changes in  $f_{cc}$  and  $\varepsilon_{cc}$  in the columns containing steel fibers as compared to the columns without steel fibers. Therefore, the test results of circular STCC columns with the employment of UHPC and UHPFRC were analyzed together.

### 3. Proposed formulae for predicting $f_{cc}$ and $\varepsilon_{cc}$

The database of the test results of circular STCC employing UHPC and UHPFRC reported by Schneider (2006), Xiong (2012), An and Fehling (2017a, b, c) was collected and shown in Table 3. The test data in the database were sorted into two groups including short and intermediate columns. The previous studies on STCC columns suggested that the increase in the confinement index  $\xi$  would significantly increase the confined peak stress  $f_{cc}$  and its corresponding strain  $\varepsilon_{cc}$ . Expressions for predicting  $f_{cc}$  and  $\varepsilon_{cc}$  can be obtained from the regression analysis on the relationship between  $f_{cc}/f_c$  and  $\xi$ ; between  $\varepsilon_{cc}/\varepsilon_c$  and  $\xi$  for the short columns as illustrated in Fig. 1

$$f_{cc} = 0.92 f_c \cdot e^{1.04\xi} \quad (10)$$

$$\varepsilon_{cc} = 3.38 \varepsilon_c \cdot \xi^{0.54} \quad (11)$$

In the case of UHPC and UHPFRC, regardless of steel fibers, the peak strain at the peak strength of concrete cylinder can be estimated using the equation proposed by An and Fehling (2017f)

$$\varepsilon_c = 0.0257 f_c^{0.96} \quad (12)$$

Similarly, the regression analysis on the relationship between  $f_{cc}/f_c$  and  $\xi$ ;  $\varepsilon_{cc}/\varepsilon_c$  and  $f_{cc}/f_c$  for the intermediate columns as depicted in Fig. 2 resulted in the development of equations to predict  $f_{cc}$  and  $\varepsilon_{cc}$

$$f_{cc} = 0.88 f_c \cdot e^{0.94\xi} \quad (13)$$

$$\varepsilon_{cc} = \varepsilon_c \left( 0.8 \cdot \ln \frac{f_{cc}}{f_c} + 1.5 \right) \quad (14)$$

### 4. Assessment of different empirical formulae

The comparison of the predictions of  $f_{cc}$  and  $\varepsilon_{cc}$  obtained from previous empirical models as shown in Tables 4-6 and the developed formulae (Eqs. (10)-(14)) with the test results was conducted in order to evaluate their prediction accuracy. Tables 4-6 show the comparison between the predictions and the test results for the short columns and the intermediate columns. To supplement these tables and make these comparisons more meaningful, the graphical comparison is also depicted in Figs. 3(a)-(b). The ratios of  $f_{cc,pre}/f_{cc,test}$  and  $\varepsilon_{cc,pre}/\varepsilon_{cc,test}$  were calculated for the comparisons between the predictions and the test results, in which  $f_{cc,pre}$  and  $\varepsilon_{cc,pre}$  denoted the values of  $f_{cc}$  and  $\varepsilon_{cc}$  obtained from the predictions, respectively;  $f_{cc,test}$  and  $\varepsilon_{cc,pre}$  referred to the values of  $f_{cc}$  and  $\varepsilon_{cc}$  obtained from the actual tests, respectively.

It is evident from Tables 4-5 that for the short columns,

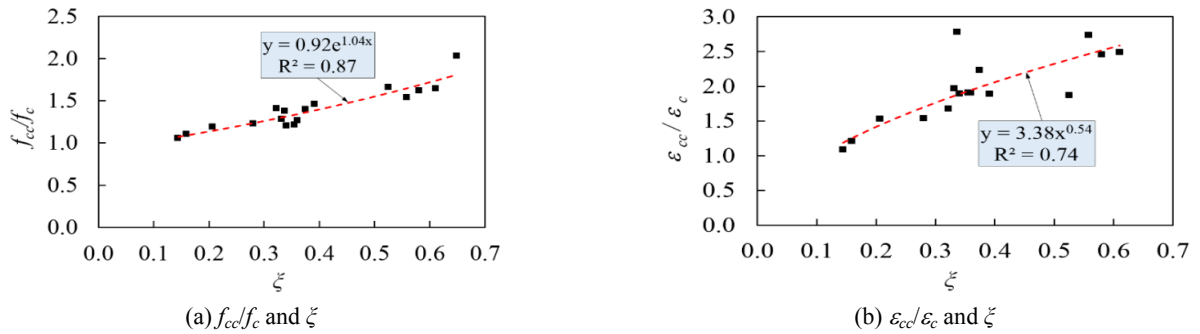


Fig. 1 Regression analysis on the relationship between: (a)  $f_{cc}/f_c$  and  $\xi$ ; (b)  $\varepsilon_{cc}/\varepsilon_c$  and  $\xi$  for the short columns

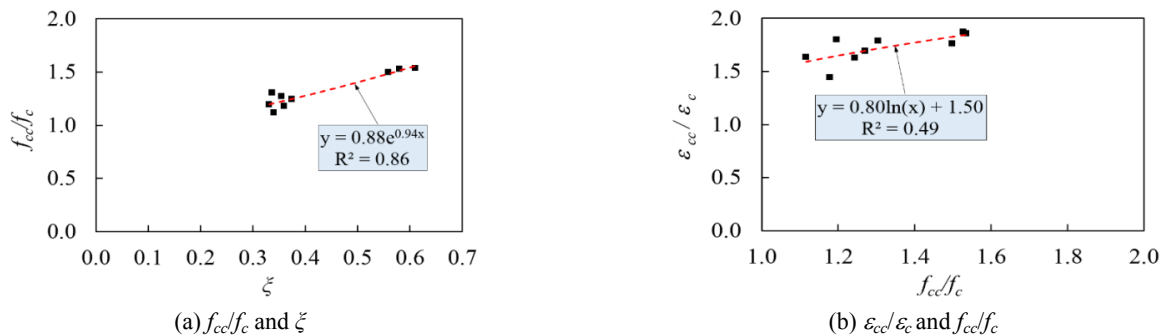


Fig. 2 Regression analysis on the relationship between: (a)  $f_{cc}/f_c$  and  $\xi$ ; (b)  $\varepsilon_{cc}/\varepsilon_c$  and  $f_{cc}/f_c$  for the intermediate columns

Table 4 Comparison of  $f_{cc}$  between the predictions of empirical formulae and the test results for the short columns

Specimens	$\xi$	$f_{cc,test}$ (MPa)	$f_{cc,pre} / f_{cc,test}$							
			Yu <i>et al.</i> (2010)	Yamamoto <i>et al.</i> (2000)	Ding <i>et al.</i> (2011)	Liu <i>et al.</i> (2016)	De Oliveira <i>et al.</i> (2010)	Guo (2014)	O'Shea and Bridge (2000)	This study Eq. (10)
SF0-t50-L600	0.34	229.04	1.33	1.24	1.31	1.29	1.08	1.63	1.13	1.08
SF1-t50-L600	0.33	251.13	1.23	1.15	1.22	1.19	1.01	1.51	1.05	1.00
SF2-t50-L600	0.34	265.36	1.15	1.08	1.14	1.12	0.94	1.41	0.98	0.94
SF0-t63-L600	0.36	240.70	1.33	1.24	1.32	1.28	1.08	1.63	1.13	1.08
SF1-t63-L600	0.36	248.20	1.28	1.20	1.27	1.24	1.04	1.57	1.09	1.04
SF2-t63-L600	0.37	262.87	1.17	1.10	1.17	1.14	0.95	1.45	1.00	0.96
SF0-t88-L600	0.61	294.50	1.19	1.15	1.24	1.17	0.95	1.49	1.00	1.04
SF1-t88-L600	0.56	300.65	1.23	1.18	1.27	1.21	0.98	1.54	1.03	1.06
SF2-t88-L600	0.58	305.24	1.18	1.14	1.22	1.16	0.94	1.48	0.99	1.03
NB2.5-UHFB	0.14	175.97	1.26	1.12	1.18	1.18	1.03	1.46	1.09	1.00
NB3.0-UHFB	0.16	183.99	1.23	1.08	1.15	1.15	1.00	1.43	1.06	0.97
NB4.0-UHFB	0.21	207.71	1.19	1.07	1.13	1.12	0.97	1.41	1.02	0.95
NB4.8-UHFB	0.28	217.09	1.23	1.13	1.20	1.18	1.00	1.50	1.05	0.99
NB5.0-UHFB	0.32	239.69	1.12	1.04	1.10	1.08	0.90	1.37	0.95	0.91
NB5.6-UHFB	0.39	253.49	1.14	1.07	1.14	1.11	0.91	1.41	0.96	0.94
NB8.0-UHFB	0.53	290.07	1.11	1.06	1.14	1.10	0.88	1.39	0.94	0.95
S1-2-1(a)*	0.65	352.99	0.99	0.98	1.03	0.98	0.88	1.24	0.83	0.88
Mean value			<b>1.198</b>	<b>1.119</b>	<b>1.191</b>	<b>1.159</b>	<b>0.973</b>	<b>1.465</b>	<b>1.018</b>	<b>0.989</b>
Coefficients of variation (COV)			<b>0.070</b>	<b>0.064</b>	<b>0.064</b>	<b>0.064</b>	<b>0.063</b>	<b>0.067</b>	<b>0.075</b>	<b>0.061</b>

Table 5 Comparison of  $\varepsilon_{cc}$  between the predictions of empirical formulae and the test results for the short columns

Specimens	$\xi$	$\varepsilon_{cc,test}$ (‰)	$\varepsilon_{cc,pre} / \varepsilon_{cc,test}$			
			Guo (2014)	Ding <i>et al.</i> (2011)	O'Shea and Bridge (2000)	This study Eq. (11)
SF0-t50-L600	0.34	7.51	0.67	1.18	0.54	1.00
SF1-t50-L600	0.33	8.01	0.64	1.09	0.52	0.95
SF2-t50-L600	0.34	11.13	0.46	0.79	0.37	0.68
SF0-t63-L600	0.36	7.84	0.68	1.19	0.55	1.02
SF1-t63-L600	0.36	7.74	0.69	1.21	0.55	1.02
SF2-t63-L600	0.37	8.74	0.60	1.09	0.47	0.89
SF0-t88-L600	0.61	9.30	0.72	1.55	0.42	1.04
SF1-t88-L600	0.56	11.13	0.62	1.24	0.39	0.90
SF2-t88-L600	0.58	9.62	0.71	1.46	0.43	1.03
NB2.5-UHFB	0.14	3.80	0.74	1.17	0.93	1.09
NB3.0-UHFB	0.16	4.22	0.70	1.12	0.84	1.04
NB4.0-UHFB	0.21	5.57	0.63	1.04	0.67	0.94
NB4.8-UHFB	0.28	5.67	0.74	1.29	0.67	1.11
NB5.0-UHFB	0.32	5.99	0.74	1.35	0.61	1.09
NB5.6-UHFB	0.39	6.84	0.73	1.39	0.55	1.08
NB8.0-UHFB	0.53	6.84	0.87	1.82	0.56	1.28
Mean value			<b>0.684</b>	<b>1.248</b>	<b>0.566</b>	<b>1.009</b>
Coefficients of variation (COV)			<b>0.129</b>	<b>0.188</b>	<b>0.272</b>	<b>0.127</b>

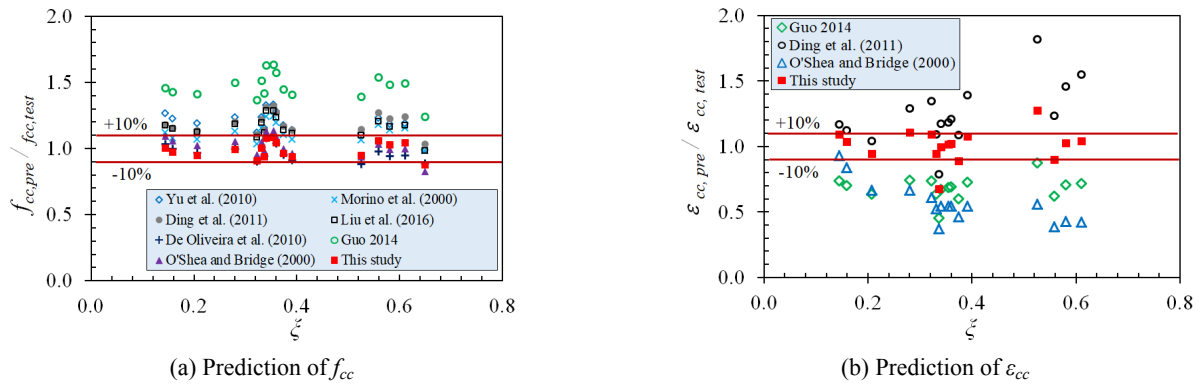


Fig. 3 Comparison of predictions by the empirical and proposed formulae with test results for the short columns

the developed equations gave the most accurate prediction of  $f_{cc}$  with a slight underestimation of 1.1% and a COV of 6.1%. As seen from Table 4, in comparison with the test results of  $f_{cc}$ , the formula by De Oliveira *et al.* (2010) slightly underestimated the value of  $f_{cc}$ , while the formula by O'Shea and Bridge (2000) performed a slight overestimation. The prediction of  $f_{cc}$  by the formulae proposed by De Oliveira *et al.* (2010) and O'Shea and Bridge (2000) were much close to the test results with average differences of 2.8% and 1.8%, COVs of 6.3% and 7.5%, respectively. Therefore, in addition to the new developed formulae, the formulae by De Oliveira *et al.* (2010) and O'Shea and Bridge (2000) can be reliably used for the prediction of  $f_{cc}$  in the short columns. In contrast, the rest of the formulae presented a substantial overestimation of  $f_{cc}$  as compared to the test results with very high mean values of  $f_{cc,pre}/f_{cc,test}$  as shown in Table 4. The accuracy of the prediction from empirical formulae could be explained by the fact that the proposed formulae by De Oliveira *et al.* (2010), and O'Shea and Bridge (2000) were derived from the tests encompassing a wide range of concrete strengths up to 120 MPa, whereas the other formulae were extracted from the tests on the columns with using only NSC.

In terms of the confined peak strain  $\epsilon_{cc}$ , Table 5 shows that the proposed formulae by Guo (2014) and O'Shea and

Bridge (2000) largely underestimated the values of  $\epsilon_{cc}$  with large scatters in their predictions, while the prediction of Ding *et al.* (2011) was much higher than the test results with an average difference of 24.8% and with a relatively large scatter COV of 18.8%. Therefore, these empirical formulae are mostly becoming unreliable to predict the confined peak strain  $\epsilon_{cc}$ . However, the prediction by the developed formula (Eq. (11)) gave a more consistent prediction than other empirical formulae in Table 2. The values of  $\epsilon_{cc}$  computed by the developed formula were close to the test results and the mean value of  $\epsilon_{cc,pre}/\epsilon_{cc,test}$  was very close to unity (1.009). Furthermore, the developed formula performed a relatively small variability in its individual prediction for each test specimen with COV of 12.7%.

With respect to the intermediate columns, only the predictions of the confined peak stress  $f_{cc}$  were compared with the test results because there were no available formulae proposed by previous studies for estimating the confined peak strain  $\epsilon_{cc}$  for the intermediate columns. Table 6 demonstrates the comparison of  $f_{cc}$  obtained from the proposed formula by De Oliveira *et al.* (2010) and the Eq. (13) in this study with the actual test results. As clearly shown in this table, the value of  $f_{cc}$  was slightly underestimated by average 5.3% by the proposed formula in

Table 6 Comparison of  $f_{cc}$  between the predictions of empirical formulae and the test results for the intermediate columns

Specimens	$\xi$	$f_{cc,test}$ (MPa)	De Oliveira <i>et al.</i> (2011)		This study Eq. (13)	
			$f_{cc,pre}$ (MPa)	$f_{cc,pre}/f_{cc,test}$	$f_{cc,pre}$ (MPa)	$f_{cc,pre}/f_{cc,test}$
SF0-t50-L1000	0.34	212.55	222.22	1.05	230.75	1.09
SF1-t50-L1000	0.33	233.95	226.66	0.97	235.04	1.00
SF2-t50-L1000	0.34	251.02	223.92	0.89	232.40	0.93
SF0-t63-L1000	0.36	251.67	233.70	0.93	243.32	0.97
SF1-t63-L1000	0.36	230.43	231.58	1.00	241.28	1.05
SF2-t63-L1000	0.37	233.65	225.22	0.96	235.01	1.01
SF0-t88-L1000	0.61	274.80	251.22	0.91	279.45	1.02
SF1-t88-L1000	0.56	292.95	265.21	0.91	290.86	0.99
SF2-t88-L1000	0.58	287.42	259.28	0.90	285.76	0.99
Mean values				<b>0.947</b>		<b>1.004</b>
Coefficients of variation (COV)				<b>0.055</b>		<b>0.045</b>

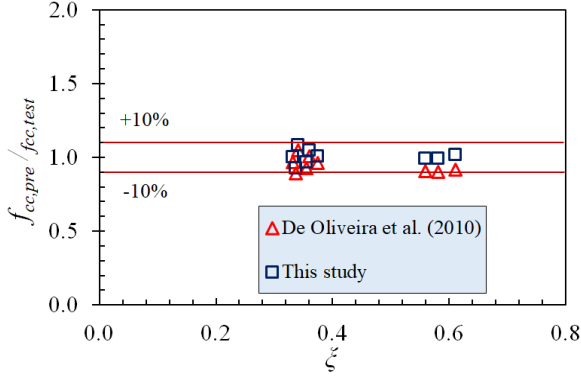


Fig. 4 Comparison of predictions of  $f_{cc}$  by the empirical and proposed formulae with test results for the intermediate columns

De Oliveira *et al.* (2010), while the developed formula provided a slight overestimation of approximately 0.4%. The small scatters with COV = 5.5% and 4.5% were also noted for the predictions by De Oliveira *et al.* (2010) and the developed formula, respectively. Hence, both the formula proposed by De Oliveira *et al.* (2010) and the developed formula (Eq. (13)) can be applicable to predict the confined peak stress  $f_{cc}$ . Fig. 4 shows the graphical comparison of the prediction of  $f_{cc}$  between Eq. (13) and the model of De Oliveira *et al.* (2010) in the case of the intermediate columns.

## 5. Simplified stress-strain model for UHPC and UHPFRC confined by steel tube

Based on the observation of the test results in An and Fehling (2017a, b, c), the complete axial stress versus axial strain of UHPC and UHPFRC confined by the steel tube short and intermediate columns can be mainly defined by three portions, as shown in Fig. 5:

- The ascending part (OA) describes the elastic and elastic-plastic behavior
- The descending part (AB) depicts the loss of load capacity right after the ultimate load
- The plateau part (BC) illustrates the stabilized stage of the columns, at which the load is assumed to be constant, while the strain progressively increases. It is mentioned that, although there is a recovery stage of load in some test specimens, the magnitude of the increased load is quite small. Therefore, in order to simplify the proposed stress-strain model, the recovery stage can be neglected.

The following equation which was originally proposed by Samani and Attard (2012) and has been widely used by previous researchers to describe the axial stress-strain relationship of the confined concrete columns in the ascending branch, is adopted as part in the simplified model

$$Y = \frac{A \cdot X + B \cdot X^2}{1 + (A-2) \cdot X + (B+1) \cdot X^2} \quad \text{when } 0 \leq \varepsilon \leq \varepsilon_{cc} \quad (15)$$

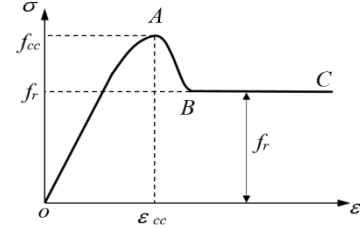


Fig. 5 Stress-strain model for UHPC and UHPFRC confined by steel tube columns

where

$$Y = \frac{\sigma}{f_{cc}} \quad \forall \quad 0 \leq Y \leq 1 \quad (16)$$

$$X = \frac{\varepsilon}{\varepsilon_{cc}} \quad \forall \quad X \geq 0 \quad (17)$$

$$A = \frac{E_c \cdot \varepsilon_{cc}}{f_c} \quad (18)$$

$$B = \frac{(A-1)^2}{0.55} - 1 \quad (19)$$

This set of equations as proposed by Samani and Attard (2012) for modeling the ascending branch in the axial stress-strain curve of confined concrete is applicable to a wide range of concrete compressive strength from 20 MPa to 130 MPa. Based on the regression analysis as shown above, the peak confined stress  $f_{cc}$  and its corresponding strain  $\varepsilon_{cc}$  of UHPC can be expressed according to Eq. (10) and Eq. (11) for the short columns, respectively; and following Eqs. (13) and (14) for the intermediate columns, respectively. The strain  $\varepsilon_c$  at the peak stress of the unconfined UHPC or UHPFRC under uniaxial compression is calculated using Eq. (12).

For estimating the values of  $E_c$ , Heimann (2013) developed an equation which can be adopted for both fine-grained UHPC and coarse-grained UHPC

$$E_c = 9350 \cdot f_c^{1/3} \quad (20)$$

For the descending part (AB) and plateau part (BC), an exponential function proposed by Binici (2005) is used and given by

$$\sigma = f_r + (f_{cc} - f_r) \exp \left[ - \left( \frac{\varepsilon - \varepsilon_{cc}}{\alpha} \right)^\beta \right] \quad \text{when } \varepsilon > \varepsilon_{cc} \quad (21)$$

in which  $f_r$  is the residual stress as shown in Fig. 5. The value of  $f_r$  can be denoted as the residual stress at the second peak load  $N_{res}$ . As a consequence,  $f_r$  is calculated using the ratio of the second peak load ( $N_{res}$ ) to concrete cross-sectional area ( $A_c$ )

$$f_r = \frac{N_{res}}{A_c} \quad (22)$$

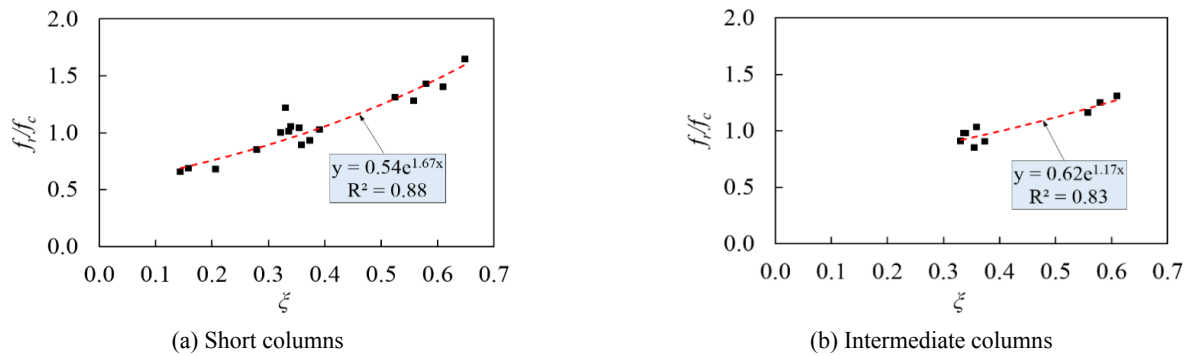


Fig. 6 Regression analysis on the relationship between the ratio  $f_r/f_c$  and  $\zeta$  for the short columns (a); and the intermediate columns (b)

The following equations for estimating  $f_r$  can be proposed by the result of regression analysis of relationships between the ratio  $f_r/f_c$  and the confinement index  $\zeta$  in Fig. 6

$$f_r = 0.54 \cdot f_c \cdot e^{1.67\zeta} \quad \text{for the short columns} \quad (23)$$

$$f_r = 0.62 \cdot f_c \cdot e^{1.17\zeta} \quad \text{for the intermediate columns} \quad (24)$$

In Eq. (21),  $\alpha$  and  $\beta$  are the parameters determining the shape of the descending part (AB). The value of  $\alpha$  is expressed following Tao *et al.* (2013)

$$\alpha = 0.04 - \frac{0.036}{1 + e^{6.08\zeta - 3.49}} \quad (25)$$

The parameter  $\beta$  controls the slope of the descending part (AB). Different trial values of  $\beta$  were adopted to find the best value which ensures the best agreement between the descending part obtained from the simplified model and the test results. The authors found that, when  $\beta$  was equal to 30 for the short columns and 10 for the intermediate columns, the predicted descending branches were acceptable compared with those in the experiments. Within the limitation of the test database, the validity of the simplified model is:  $200 \text{ MPa} \geq f_c \geq 150 \text{ MPa}$  and  $235 \leq f_y$  (MPa)  $\leq 460$ , and  $0.1 \leq \zeta \leq 0.7$ .

## 6. Verifications of the simplified stress-strain model

To further examine the accuracy of the simplified model, Figs. 7-9 compare the predictions of the simplified model with experimental stress-strain curves of the short and the intermediate columns, respectively. For the short columns, in addition to the test results reported by An and Fehling (2017a, b, c), the test results of seven columns presented in Schneider (2006) were used for validation of the simplified model, as shown in Fig. 9. In the tests conducted by An and Fehling (2017a, b, c), the axial strains in the stress-strain curves were derived from the average axial displacements measured by three linear variable differential transducers (LVDTs) divided by the concrete

length. However, in the case of tests carried out by Schneider (2006), these axial strains were directly measured over a length of 300 mm at the middle height of columns through three LVDTs. These three LVDTs were used to capture the axial displacement of steel bars, which were positioned in the concrete core through an arrangement of drillings in the steel tube. It can be seen that the method in Schneider (2006) was more complicated, but more precise than that in An and Fehling (2017a, b, c).

As evident from the comparisons, the predictions of the simplified model are globally in good agreement with the experimental results. In the case of comparison with test results in Schneider (2006), the stress-strain curves obtained from the simplified model were very close to those measured in the tests, as depicted in Fig. 9. Although the predicted curves of some columns somewhat deviate from the test curves (e.g., the columns SF0-t5.0-L600, SF2-t5.0-L600), the general shape is quite similar. However, the distinctive discrepancy between the measured results and the simplified model predictions is concerned with the initial slope of the ascending branch. As explained in the previous studies by An and Fehling (2007b), the interfacial slip due to the debonding occurs at the initial loading stage within about 25 MPa. As a result, the initial stiffness is reduced and the slope of the axial stress-axial strain curves is smaller. This phenomenon is extremely complicated to be included into the simplified model. Furthermore, the interfacial slip, in other words, the bonding resistance between the concrete core and the steel tube might be varied among the columns. For these reasons, the simplified model did not account for the interfacial slip, thereby causing the fact that the predicted and measured ascending branches were not close to each other. It can be seen that a larger interfacial slip or smaller slope after debonding lead to a decrease in the deviation between the predicted and measured ascending branches (e.g., the columns SF0-t8.8-L600, SF1-t8.8-L600, SF0-t5.0-L600, SF1-t5.0-L600, SF2-t5.0-L600). It is also worth noting that the intermediate columns exhibited a better agreement between the predicted and measured ascending branches as compared to the short columns. This can be due to the fact that the interfacial slip in the short columns was greater than that in the intermediate columns. The slope of the ascending parts in the test curves after debonding were found to be similar to that in the predicted curves (the predicted curves were

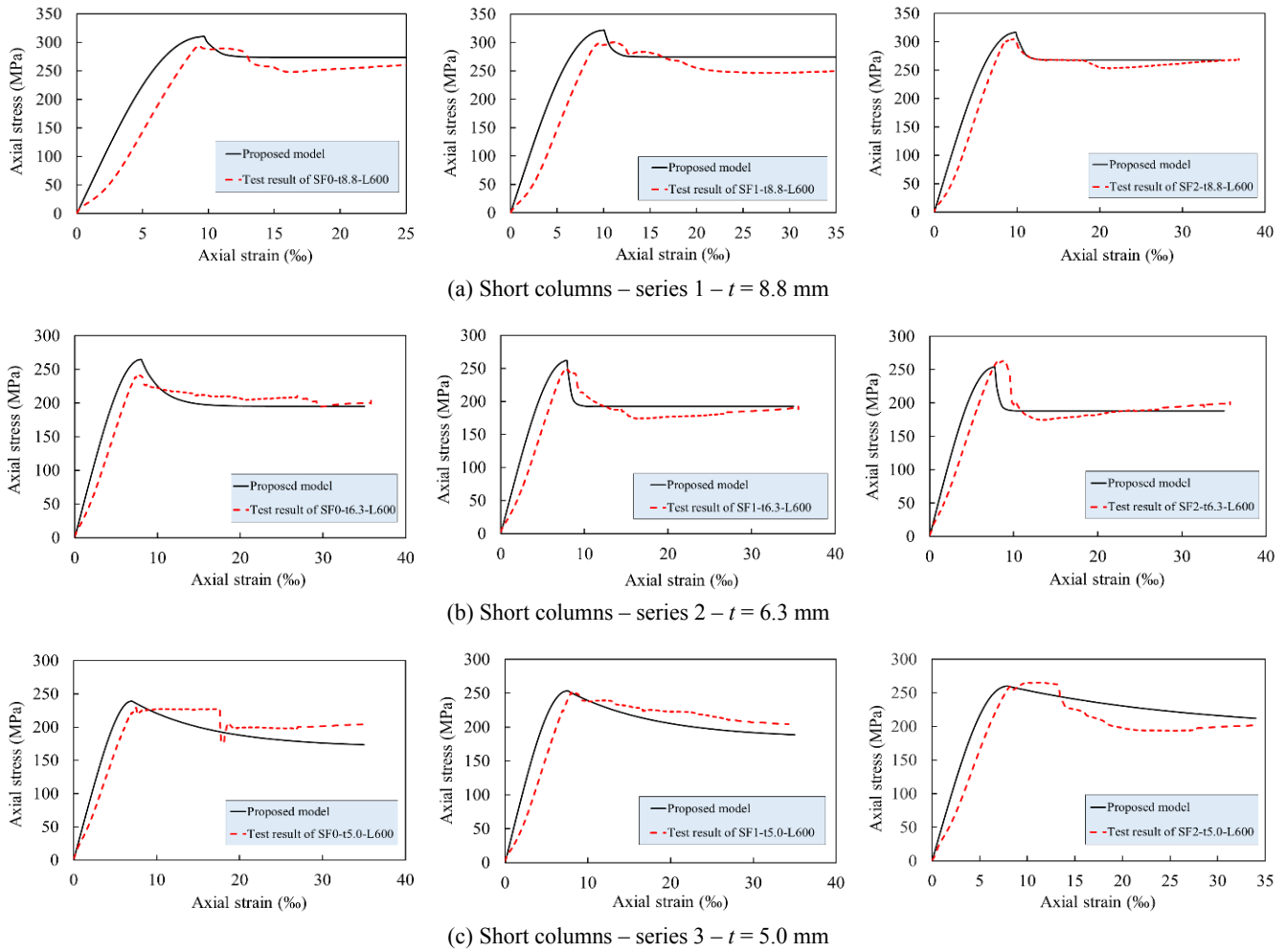


Fig. 7 Comparison of stress-strain curves of the short columns between the simplified model and test results of An and Fehling (2017a, b, c)

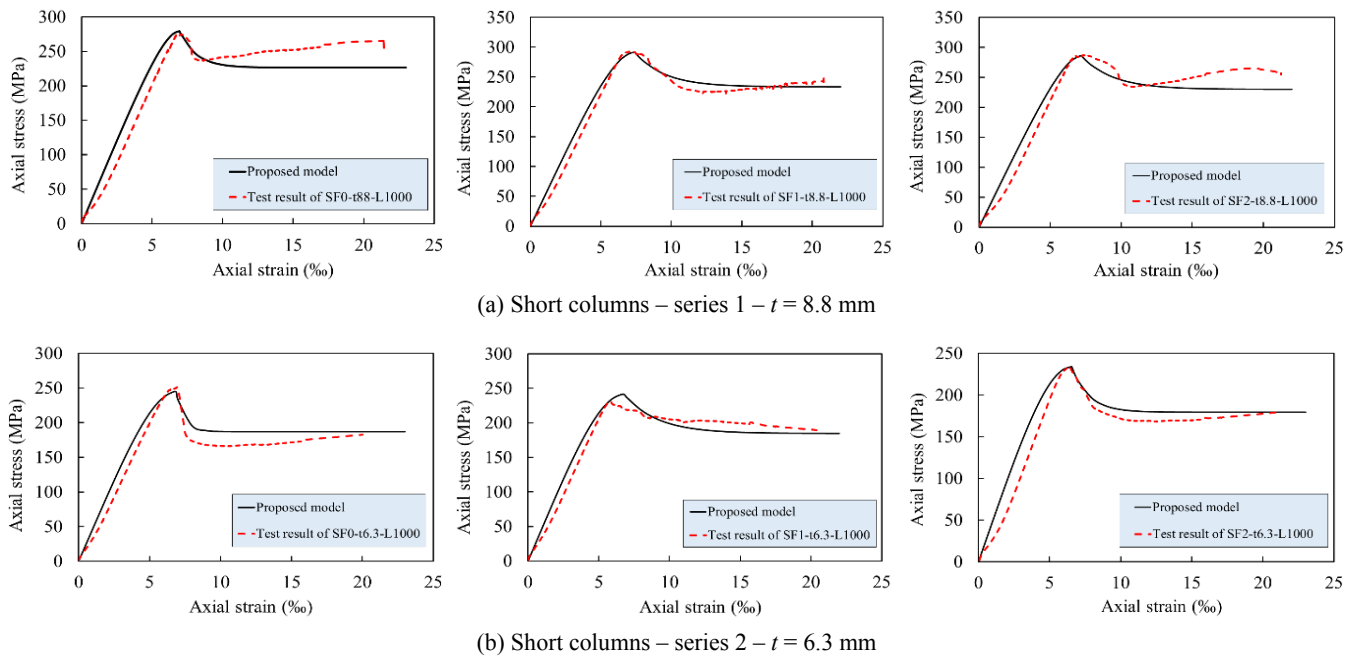


Fig. 8 Comparison of stress-strain curves of the intermediate columns between the simplified model and test results of An and Fehling (2017a, b, c)

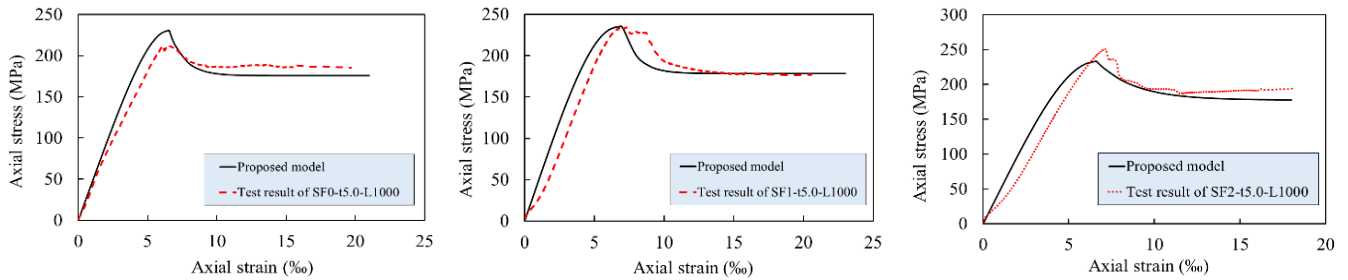
(c) Intermediate columns – series 3 –  $t = 5.0$  mm

Fig. 8 Continued

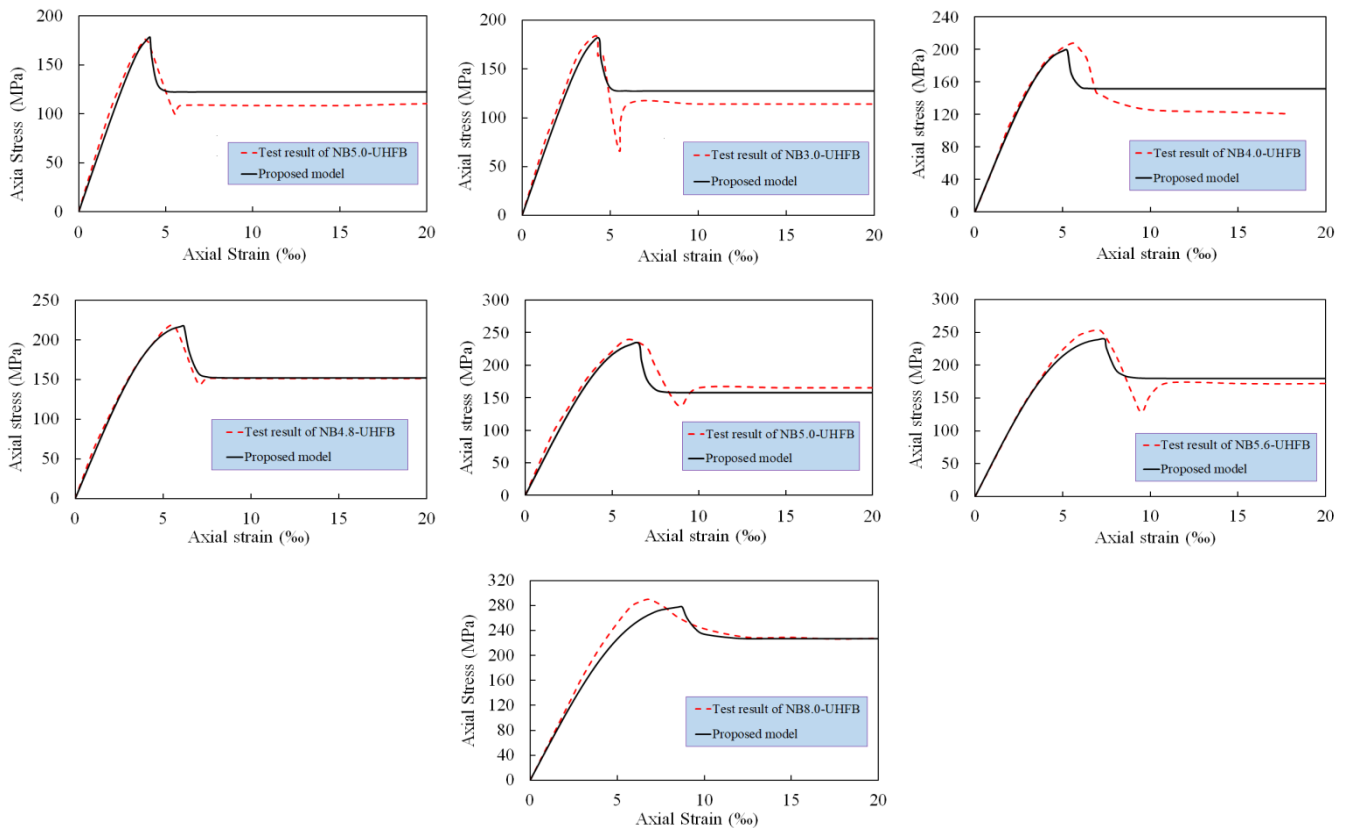


Fig. 9 Comparison of stress-strain curves of the short columns between the simplified model and test results of Schneider (2006)

likely parallel to the experimental curves after debonding), thus indicating that the stiffness of the elastic stage in the stress-strain curves generated by the simplified model is in accordance with that measured in the actual tests.

The predicted post-peak branch can reflect the general trend in the axially compressive behavior of the columns as in the actual test, although in some cases it seems that the predictions somewhat deviate from the experimental curves, especially in the short columns with a prolonged elastic-plastic stage (e.g., the columns SF0-t5.0-L600, SF1-t5.0-L600, SF0-t8.8-L600 and SF1-t8.8-L600). In brief, the simplified model gave a reasonably good prediction of the experimental stress-strain curves, thereby stating that it can be simply used for the practical design. Nevertheless, the debonding in the initial loading reinforces the importance of the bonding resistance between the concrete core and the

steel tube, which is believed to significantly affect to the behavior of the circular STCC columns. This point of view was strongly supported by some previous studies such as Johansson (2002), Liu *et al.* (2016) and Ding *et al.* (2017). The simplified model was established by the limited database of 26 tested specimens and did not consider the effect of the bonding resistance between two materials. Therefore, further experimental research on circular STCC columns with UHPC and UHPFRC infilled, and the development of UHPC and UHPFRC-specific confinement model are recommended. Much more work is also needed to investigate the influence of the bonding resistance in this column type. Moreover, the simplified model can be easily used by design engineers to predict the overall axial stress-axial strain curves and to conduct further parametric analysis on the axially compressive behavior of circular

STCC-UHPC and STCC-UHPC columns.

## 7. Conclusions

This paper has developed a simplified stress – strain model for STCC-UHPC and STCC-UHPFRC, in which the compressive strength of concrete cylinder is higher than 150 MPa. Through the current investigation, the following conclusions can be obtained:

- The formulae for predicting the confined peak stress  $f_{cc}$  and strain  $\varepsilon_{cc}$  were proposed for stub and intermediate columns based on the regression analysis of the test results reported by previous studies. As revealed by the results of the prediction assessment, the proposed formulae are more accurate than any of the existing empirical formulae in predicting  $f_{cc}$  and  $\varepsilon_{cc}$ .
- In terms of STCC-UHPC and STCC-UHPFRC short columns, the empirical formulae proposed by De Oliveira *et al.* (2010) and O’Shea and Bridge (2000) can be reliably used for predicting the confined peak stress  $f_{cc}$ , while the existing empirical formulae gave an unaccurate prediction of the confined peak strain  $\varepsilon_{cc}$ .
- In terms of STCC-UHPC and STCC-UHPFRC intermediate columns, only the formula proposed by De Oliveira *et al.* (2010) is the most appropriate model for predicting the confined peak stress  $f_{cc}$ .
- A simplified stress-strain model for circular STCC columns with the use of UHPC and UHPFRC was developed. The simplified model was found to be in very good agreement with the experimental results.

## Acknowledgments

The authors would like to acknowledge the financial support from Ton Duc Thang University, Duy Tan University, Sejong University, and Kassel University.

## References

- Aboutaha, R.S. and Machado, R. (1998), “Seismic resistance of steel confined reinforced concrete (SCRC) columns”, *Struct. Des. Tall Build.*, **7**, 251-260.
- An, L.H. and Fehling, E. (2017a), “Effect of steel fiber on the behavior of circular steel tube confined UHPC columns under axial loading”, *Proceedings of the 4th International Conference on Strain-Hardening Cement-Based Composites (SHCC4)*, Dresden, Germany, September.
- An, L.H. and Fehling, E. (2017b), “Experimental study on the compressive behavior of circular steel tube confined UHPC columns”, *Proceedings of the 16th International Symposium on Tubular Structures (ISTS16)*, Monash, Australia, December.
- An, L.H. and Fehling, E. (2017c), “Test on circular steel tube confined UHPC columns under axial loading”, *Proceedings of the 3rd International Symposium on Ultra-High Performance Fiber-Reinforced Concrete, UHPFRC 2017 Montpellier*, France, October.
- An, L.H. and Fehling, E. (2017d), “Analysis of circular steel tube confined UHPC stub columns”, *Steel Compos. Struct., Int. J.*, **23**(6), 669-682.
- An, L.H. and Fehling, E. (2017e), “Assessment of axial stress-strain model for UHPC confined by circular steel tube stub columns”, *Struct. Eng. Mech., Int. J.*, **3**(3), 371-384.
- An, L.H. and Fehling, E. (2017f), “Influence of steel fiber content and type on the uniaxial tensile and compressive behavior of UHPC”, *Constr. Build. Mater.*, **153**, 790-806.
- An, L.H. and Fehling, E. (2017g), “Numerical study of circular steel tube confined concrete (STCC) stub columns with various concrete strengths”, *J. Constr. Steel Res.*, **136**, 238-255.
- Architectural Institute of Japan (AIJ) (2001), Recommendation for design and construction of concrete filled steel tubular structures, Japan. [In Japanese]
- Binici, B. (2005), “An analytical model for stress-strain behavior of confined concrete”, *Eng. Struct.*, **27**(7), 1040-1051.
- Blais, P.Y. and Couture, M. (1999), “Precast, Prestressed Pedestrian Bridge: World’s First Reactive Powder Concrete Structure”, *PCI Journal*, **44**(5), 60-71.
- De Oliveira, W.L.A., De Nardin, S., De Cresce El Debs, A.L.H. and El Debs, M.K. (2010), “Evaluation of passive confinement in CFT columns”, *J. Constr. Steel Res.*, **66**(4), 487-495.
- Ding, F.X., Yu, Z.W., Bai, Y. and Gong, Y.Z. (2011), “Elasto-plastic analysis of circular concrete-filled steel tube stub columns”, *J. Constr. Steel Res.*, **67**, 1567-1577.
- Ding, F.X., Tan, L., Liu, X.M. and Wang, L. (2017), “Behavior of circular thin-walled steel tube confined concrete stub columns”, *Steel Compos. Struct., Int. J.*, **23**(2), 229-238.
- Ellobody, E., Young, B. and Lam, D. (2006), “Behaviour of normal and high strength concrete filled compact steel tube circular stub columns”, *J. Constr. Steel Res.*, **62**(7), 706-715.
- Fehling, E., Bunje, K. and Leutbecher, T. (2004), “Design relevant properties of hardened ultra high performance concrete”, *Proceedings of the International Symposium on Ultra High Performance Concrete*, (Eds. M. Schmidt, E. Fehling, C. Geisenhanslüke), Kassel, Germany, September, pp. 327-338.
- Fehling, E., Schmidt, M., Walraven, J., Leutbecher, T. and Fröhlich, S. (2014), *Ultra-High Performance Concrete: Fundamental – Design – Example*, Wilhelm Ernst & Sohn, Verlag für Architektur und technische Wissenschaften GmbH & Co. KG, Rotherstraße 21, 10245 Berlin, Germany.
- Giakoumelis, G. and Lam, D. (2004), “Axial capacity of circular concrete-filled tube columns”, *J. Constr. Steel Res.*, **60**(7), 1049-1068.
- Graybeal, B.A. (2005), “Characterization of the behavior of ultra-high performance concrete”, Ph.D. Dissertation; University of Maryland, USA.
- Guo, Z. (2014), *Principle of Reinforced Concrete*. ISBN: 9780128008591
- Han, L.H., Yao, G.H., Chen, Z.P. and Yu, Q. (2005), “Experimental behavior of steel tube confined concrete (STCC) columns”, *Steel Compos. Struct., Int. J.*, **5**(6), 459-84.
- Han, L.H., Liu, W. and Yang, Y.F. (2008), “Behavior of thin walled steel tube confined concrete stub columns subjected to axial local compression”, *Thin-Wall. Struct.*, **46**, 155-164.
- Han, L.H., Li, W. and Bjorhovde, R. (2014), “Development and advanced applications of concrete-filled steel tubular (CFST) structures: members”, *J. Constr. Steel Res.*, **100**, 211-228.
- Heimann, M. (2013), “Tragwerkszuverlässigkeit hochbeanspruchter Druckglieder aus ultrahochfestem Beton”, Ph.D. Dissertation; Helf 28, Technische Universität Darmstadt.
- Huang, F., Yu, X. and Chen, B. (2012), “The structural performance of axially loaded CFST columns under various loading conditions”, *Steel Compos. Struct., Int. J.*, **13**(5), 451-471.
- Johansson, M. (2002), “Composite Action and Confinement

- Effects in Tubular Steel-Concrete Columns”, Ph.D. Dissertation; Department of Structural Engineering, Concrete Structures, Chalmers University of Technology, Göteborg, Sweden.
- Liew, J.Y.R. and Xiong, D.X. (2010), “Experimental investigation on tubular columns infilled with ultra-high strength concrete”, *Tubular Structures XIII*, The University of Hong Kong, pp. 637-645.
- Liew, J.Y.R. and Xiong, D.X. (2012), “Ultra-high strength concrete filled composite columns for multi-storey building construction”, *Adv. Struct. Eng.*, **15**(9), 1487-1503.
- Liew, J.Y.R. and Xiong, D.X. (2015), *Design Guide For Concrete Filled Tubular Members With High Strength Materials to Eurocode 4*, Research Publishing, Blk 12 Lorong Bakar Batu, 349568 Singapore.
- Liew, J.Y.R., Xiong, M.X. and Xiong, D.X. (2014), “Design of high strength concrete filled tubular columns for tall buildings”, *Int. J. High-Rise Build.*, **3**(3), 215-221.
- Liew, J.Y.R., Xiong, M.X. and Xiong, D.X. (2016), “Design of concrete filled tubular beam-columns with high strength steel and concrete”, *Structures*, **8**, 215-221.
- Liu, J., Zhang, S., Zhang, X. and Guo, L. (2009), “Behavior and strength of circular tube confined reinforced-concrete (CTRC) columns”, *J. Constr. Steel Res.*, **65**, 1447-1458.
- Liu, J., Zhou, X. and Gan, D. (2016), “Effect of friction on axially loaded stub circular tubed columns”, *Adv. Struct. Eng.*, **19**(3), 546-559.
- O’Shea, M.D. and Bridge, R.Q. (1994), “Test of thin-walled concrete-filled steel tubes”, *Proceedings of the 12th International Specialty Conference on Cold-Formed Steel Structures*, St. Louis, MO, USA, October, pp. 399-419.
- O’Shea, M.D. and Bridge, R.Q. (2000), “Design of circular thin-walled concrete filled steel tubes”, *J. Struct. Eng.*, ASCE, **126**(11), 1295-1303.
- Qi, H., Guo, L., Liu, J., Gan, D. and Zhang, S. (2011), “Axial load behavior and strength of tubed steel reinforced-concrete (SRC) stub columns”, *Thin-Wall. Struct.*, **49**, 1141-1150.
- Richart, F.E., Brandzaeg, A. and Brown, R.L. (1928), “A Study of the Failure of Concrete under Combined Compressive Stresses”, Bulletin No. 185; University of Illinois, Engineering Experimental Station, Urbana, IL, USA.
- Richart, F.E., Brandzaeg, A. and Brown, R.L. (1929), “Failure of plain and spirally reinforced concrete in compression”, Bulletin 190; University of Illinois Engineering Experimental Station, Champaign, IL, USA.
- Samani, A.K. and Attard, M.M. (2012), “A stress-strain model for uniaxial and confined concrete under compression”, *Eng. Struct.*, **41**, 335-349.
- Schneider, H. (2006), “Zum tragverhalten kurzer, umschnürter, kreisförmiger, druckglieder aus ungefasertem UHFB”, Ph.D. Dissertation; University of Leipzig, Leipzig, Germany. [In German]
- Tao, Z., Wang, Z.B. and Yu, Q. (2013), “Finite element modeling of concrete filled steel stub columns under axial compression”, *J. Constr. Steel Res.*, **89**, 121-131.
- Tue, N.V., Schneider, H., Simesch, G. and Schmidt, D. (2004a), “Bearing capacity of stub columns made of NSC, HSC and UHPC confined by a steel tube”, *Proceedings of the 1st International Symposium on Ultra High Performance Concrete*, Kassel, Germany, March, pp. 339-350.
- Tue, N.V., Küchler, M., Schenck, G. and Jürgen, R. (2004b), “Application of UHPC filled tubes in buildings and bridges”, *Proceeding of International Symposium on Ultra High Performance Concrete*, Kassel, Germany, March, pp. 807-817.
- Xiong, D.X. (2012), “Structural behaviour of concrete filled steel tube with high strength materials”, Ph.D. Dissertation; National University of Singapore, Singapore.
- Xiong, M.X., Xiong, D.X. and Liew, J.Y. (2017), “Axial performance of short concrete filled steel tubes with high-and ultra-high-strength materials”, *Eng. Struct.*, **136**, 494-510.
- Yamamoto, T., Kawaguchi, J. and Morino, S. (2000), “Experimental study of scale effects on the compressive behavior of short concrete-filled steel tube columns”, *Proceeding of the 14th International Conference on Composite Construction in Steel and Concrete*, Banff, Alberta, Canada, pp. 879-890.
- Yu, Q., Tao, Z., Liu, W. and Chen, Z.B. (2010), “Analysis and calculations of steel tube confined concrete (STCC) stub columns”, *J. Constr. Steel Res.*, **66**(1), 53-64.
- Zhong, S.T. and Miao, R.Y. (1988), “Stress-Strain Relationship and Strength of Concrete Filled Tubes”, *Proceeding of Engineering Foundation Conference on Composite Constructions*, Henniker, NH, USA, pp. 773-785.

DL